Presented at the 36th European PV Solar Energy Conference and Exhibition, 9-13 September 2019, Marseille, France

ACCURATE MEASUREMENT OF BIFACIAL SOLAR CELLS WITH SINGLE- AND BOTH-SIDED ILLUMINATION

Michael Rauer, Fan Guo, Jochen Hohl-Ebinger
Fraunhofer Institute for Solar Energy Systems (ISE)
Heidenhofstraße 2, 79110 Freiburg, Germany

Corresponding author: Phone: +49(0)761/4588-5564, E-mail: michael.rauer@ise.fraunhofer.de

ABSTRACT: In order to quantify the bifaciality of bifacial solar devices in a standardized way, the IEC technical specification 60904-1-2 defines two different measurement methods that can be conducted in addition to measurements at standard testing conditions. The first method (referred to as *bifacial method*) is based on simultaneous front and rear side illumination, the second method (referred to as *equivalent irradiance (G_E) method*) comprises front-side illumination with increased irradiance. Intrinsic differences between the two methods can arise from the different photogeneration depth profiles for bifacial solar devices with *e.g.* injection-dependent recombination or inversion layer shunting. These injection-dependent effects occur as nonlinearity of short-circuit current as a function of irradiance. In this paper, the bifacial and G_E methods are compared for bifacial passivated emitter and rear (PERC) solar cells with very strong nonlinearity. To detect differences between the two methods with high accuracy, an advanced measurement setup and an adapted calibration procedure have been used. The measurement uncertainties of the setup have been determined by means of Monte Carlo simulations taking into account correlations between both methods. Differences in *IU* parameters between the two methods were measured to be below 0.1 $\%_{rel}$, which is clearly within the respective measurement uncertainties. The two methods presented in the IEC technical specification 60904-1-2 can therefore be considered as consistent for bifacial solar cells with respect to nonlinearity. Further measurements and simulations indicate that the consistency also holds for lower front irradiances, which are relevant for energy rating and yield assessment of bifacial devices.
Keywords: Bifacial Solar Cells, Equivalent Irradiance (G_E) Method, Standardization, IV Measurement

1 INTRODUCTION

Bifacial solar cells and modules are becoming more and more important in today's solar cell market. Due to their high energy gain, their market share is expected to increase to over 50 % in the next 10 years [1].

An essential issue which has hindered the market introduction of bifacial products was the missing standardized characterization procedures for evaluating their performance. This gap has been closed by the IEC technical specification (TS) 60904-1-2 [2], which proposes two different methods for measurements of bifacial solar cells and modules. The first method, which is referred to as *bifacial method* in the following, is based on illuminating the device with an irradiance of 1000 W/m^2 from front and simultaneously with a reduced irradiance of 100 and 200 W/m^2, respectively, from the rear. The second method, which is referred to as *equivalent irradiance (G_E) method*, comprises front-side illumination only, but with irradiance higher than 1000 W/m^2. In the TS, both methods are presented as consistent and all experiments reported so far have shown consistency between the two measurement methods with deviations in the range of 0.4 to 2 $\%_{rel}$ [3-6].

For manufacturers and investors, this is not satisfactory though, as they need to know which method is preferable for characterization of their bifacial products. Already deviations of only 1.0 % –passed to yearly worldwide solar cell production– lead to budget uncertainties in the hundred million dollar range.

From a theoretical point of view, a brief calculation proves that the bifacial and G_E methods are similar for bifacial solar cells with linear relation between short-circuit current and irradiance [7], *i.e.* for so-called *linear* solar cells. For *nonlinear* bifacial solar cells without linear current-irradiance relation, though, intrinsic differences between the two methods can result from the different photogeneration profiles: Whereas both-sided illumination leads to photogeneration at front and at rear, single-sided illumination causes generation mainly near the front. Nonlinear effects like injection-dependent bulk or surface recombination [8] or inversion layer shunting [9] can lead to differences in diffusion lengths in the bulk and in carrier collection. This can in turn result in differences between the bifacial and G_E methods. In the literature, it has therefore been recommended to always evaluate linearity of bifacial solar cells [10].

Among bifacial solar cells, nonlinearity occurs predominantly in bifacial PERC (passivated emitter and rear) solar cells with silicon nitride or silicon oxynitride rear passivation layer containing high density of positive charges. In this study, nonlinear bifacial PERC solar cells with strongly nonlinear rear recombination characteristics are measured with both bifacial and G_E methods. As there are –to the authors' knowledge– currently no bifacial solar cells available with stronger nonlinearity, this study represents a worst-case investigation.

2 EXPERIMENTAL

2.1 Bifacial Passivated and Emitter Rear Cell

Large-area bifacial *p*-type silicon solar cells with passivated rear surface and three busbars have been investigated in this study. A stack of silicon oxynitride SiO_xN_y and silicon nitride SiN_z [11] has been used for rear surface passivation. As the rear side of the solar cells is not textured [11], the bifaciality of the solar cells, given by the ratio $I_{sc,rear,STC}/I_{sc,front,STC}$ of rear to front short-circuit current measured at standard testing conditions (STC), is 61 %.

In contrast to widely used aluminium oxide/silicon nitride (AlO_x/SiN_y) passivation layers, the SiO_xN_y/SiN_z stack features a high density of positive charges [12]. It has been shown that the surface recombination velocity does not exhibit an injection dependence [11,13]. The passivation layer though introduces an inversion layer on

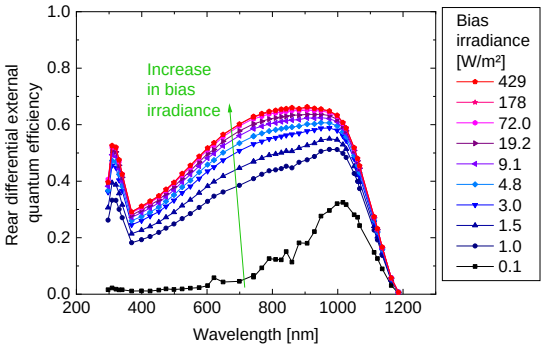

Figure 1: Differential external quantum efficiency (EQE) measured on rear side of a bifacial PERC solar cell.

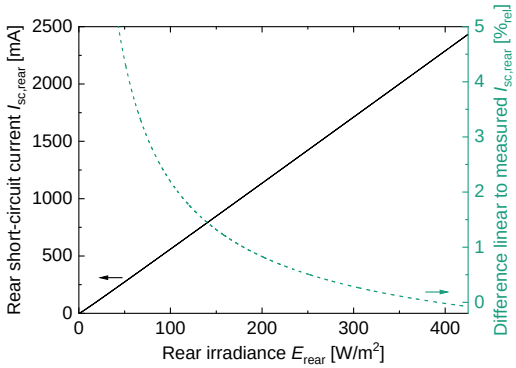

Figure 2: Rear short-circuit current $I_{sc,rear}$ as a function of rear irradiance E_{rear} determined from the differential EQE data (black line). The dashed green line shows the difference to a linear current-irradiance relation.

the rear of the solar cell which is shunted at the local aluminum-alloyed contacts. This so-called inversion layer shunting introduces an injection-dependency [9] and therefore leads to a nonlinear relation between irradiance E and short-circuit current I_{sc} of the solar cells.

2.2 Differential Spectral Responsivity Measurements

The nonlinear $I_{sc}(E)$ characteristics can be investigated well by differential spectral responsivity (DSR) measurements, which are very sensitive to linearity effects due to the differential character of the measurement procedure [14-16]. Before the investigations, light exposure was performed for 24 hours to eliminate the potential influence of boron-oxygen defects.

Figure 1 shows the differential external quantum efficiency (EQE) measured on the rear of a bifacial PERC cell at different bias irradiance levels. A non-reflective measurement chuck has been used thereby to minimize the contribution of transmitted and reabsorbed light [17,18]. It can clearly be seen that the differential EQE exhibits a strong bias dependency and increases strongly with increasing bias irradiance. As mainly the wavelength range below 1000 nm is affected by bias irradiance (*i.e.* light that is absorbed at the rear and in the base of the solar cell), it can be concluded that recombination at the rear of the solar cell is strongly injection dependent.

By weighting the differential EQEs (or the differential spectral responsivities) with the AM1.5g spectral distribution and using a well-established integration method [19], the exact relation between rear short-circuit current $I_{sc,rear}$ and rear irradiance E_{rear} can be determined, see Figure 2. Although the relation *appears* linear, the curve exhibits a rather large nonlinearity. The green dashed line shows the relative difference to linear characteristics, which were determined by the relation $I_{sc,rear,STC}/E_{rear,STC} \cdot E_{rear}$, with $I_{sc,rear,STC}$ and $E_{rear,STC}$ standing for rear short-circuit current and rear irradiance at standard testing conditions (STC), respectively.

To quantify the bifaciality of the bifacial PERC solar cell, DSR measurements have also been carried out on the front of the solar cell and the relation between front short-circuit current $I_{sc,front}$ and front irradiance E_{front} has been determined. Furthermore, calibrated current-voltage (*IU*) measurements at different irradiance levels have been performed. From both measurements, the bifaciality in short-circuit current, which is given by the ratio $I_{sc,rear}$ / $I_{sc,front}$, has been derived as a function of irradiance. Figure 3 shows that the nonlinear rear characteristics strongly affect the bifaciality of the bifacial PERC cell, as the bifaciality strongly depends on irradiance.

The bifacial PERC solar cells investigated in this study are therefore adequate and challenging test devices for comparing bifacial and G_E methods. To the authors' knowledge, there are no bifacial solar cells with more pronounced nonlinearity available at present, so that this investigation represents a worst-case study.

2.3 PC1D Model of Nonlinear Bifacial PERC Solar Cells

A PC1D model of the bifacial PERC solar cells has been set up [20], which particularly accounts for the nonlinearity caused by inversion layer shunting. Adequate accordance to measured front and rear differential EQEs has been achieved [20]. As it has been difficult to simulate both the injection-dependence of front and rear recombination in perfect agreement to measured data though, the simulation model was chosen to exhibit a slightly overrated nonlinearity and thus represents a worst case scenario. The simulated solar cell features an $I_{sc,rear,STC}$ to $I_{sc,front,STC}$ ratio of 71.6 %.

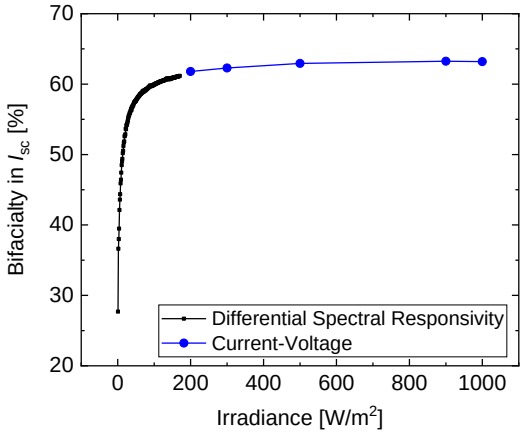

Figure 3: Bifaciality in short-circuit current, given by the ratio $I_{sc,rear}/I_{sc,front}$, as a function of irradiance determined from differential EQE data (black symbols) and current-voltage measurements (blue symbols).

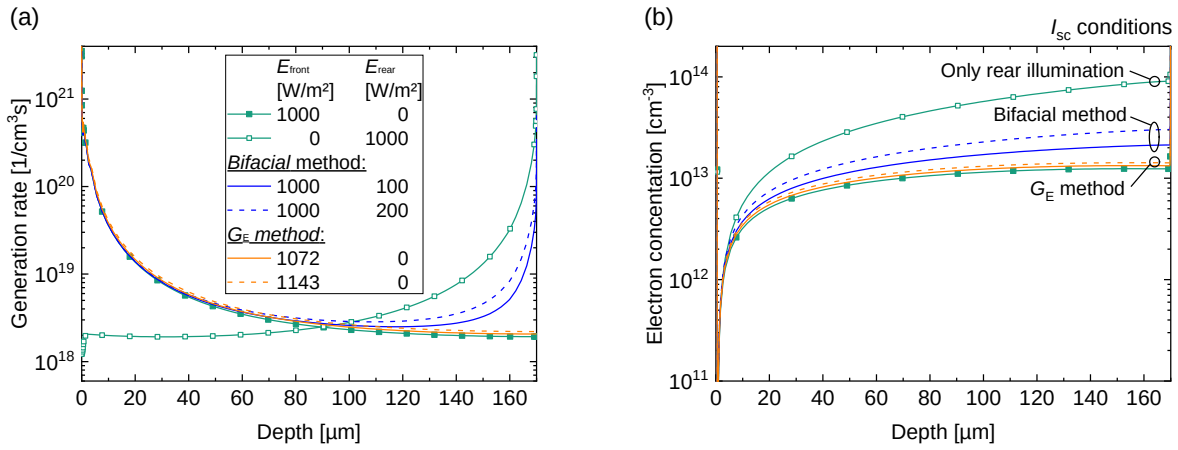

Figure 4: PC1D-simulated (a) photogeneration rate and (b) electron concentration as a function of the depth of a bifacial PERC solar cell (cell thickness 170 µm). As the bifaciality of the simulated cell is 71.6 %, the blue and orange lines for bifacial and equivalent irradiance methods represent analogous measurement conditions.

The model was used to gain improved insight into the physics of nonlinear bifacial solar cells with respect to different front and rear illumination configurations.

3 CURRENT-VOLTAGE MEASUREMENT OF BIFACIAL SOLAR CELLS

3.1 Measurement Procedures

Bifacial solar cells are commonly characterized by the current-voltage (*IU*) characteristics of front and rear side measured at STC. To further quantify the bifacial performance of the solar cells, two different advanced approaches are proposed in the IEC technical specification (TS) 60904-1-2 [2]:

1. Both-sided illumination (*bifacial method*):

Front irradiance E_{front} = 1000 W/m^2 and simultaneous rear irradiance E_{rear} = 100 and 200 W/m^2, respectively.

2. Single-sided illumination (*equivalent irradiance (G_E) method*):

Equivalent front irradiance $E_{\mathrm{E}} = 1000\ \mathrm{W/m^2} + \frac{I_{\mathrm{sc,rear,STC}}}{I_{\mathrm{sc,front,STC}}} \cdot E_{\mathrm{rear}}$ with E_{rear} = 100 and 200 W/m^2, respectively. E_{rear} represents the "compensated" rear irradiance that is added to the front side with the $I_{\mathrm{sc,STC}}$ ratio as weight.

In the TS, both approaches are considered as consistent.

3.2 Importance of Nonlinearity of Bifacial Solar Cells

The PC1D model of the bifacial PERC solar cell was used to simulate the photogeneration and electron concentration depth profiles in the cell for the bifacial and the equivalent irradiance methods introduced in the previous section (see Figure 4). It is clearly visible that the photogeneration profiles are intrinsically different.

The differences in the photogeneration profiles can be critical if injection-dependent effects occur: For calculating the equivalent front irradiance, the I_{sc} ratio at 1000 W/m^2 is used. As particularly the depth profile of photogeneration with only rear illumination (open green symbols) differs significantly from the profile of photogeneration with equivalent and bifacial illumination conditions (orange or blue lines), different electron concentration profiles in the base and at the rear surface occur, see Figure 4 (b). Injection-dependent effects, *e.g.* an injection-dependent rear surface recombination velocity or inversion layer shunting, can lead to different electron diffusion lengths and, thus, to differences in carrier collection between these illumination conditions.

As surface recombination velocity commonly decreases and inversion layer shunting diminishes with increasing injection level [8,9], the $I_{\mathrm{sc,rear}}$ determination with rear irradiance of 1000 W/m^2 is carried out with overestimated electron concentration at the rear and thus with underestimated surface recombination. As a consequence, the $I_{\mathrm{sc,rear}}$ to $I_{\mathrm{sc,front}}$ ratio at 1000 W/m^2 is overrated and the equivalent irradiance, which is calculated from this ratio, is overrated as well. As a consequence, the I_{sc} determined with the equivalent irradiance method is higher than the one determined with the bifacial method for the E_{rear} conditions specified by the IEC technical specification.

In *IU* measurements, injection-dependent effects lead to nonlinearity of short-circuit current as a function of irradiance. These so-called nonlinear solar cells can therefore exhibit intrinsic differences between the *IU* characteristics measured with bifacial and G_{E} methods as a result of the different photogeneration depth profiles.

3.3 Two-Mirror Setup at CalLab PV Cells

To be able to detect differences between the methods with highest accuracy, an advanced measurement setup as well as the precise knowledge of its measurement uncertainty is crucial. In this study, a setup with one light source and two mirrors as proposed by [21,22] is used to realize single- and both-sided illumination [20].

The solar cell is placed vertically between two tilted mirrors, which reflect light of a xenon flash lamp to the front and rear sides of the solar cell (see Figure 5). For one-sided illumination, only the front light path is opened. For both-sided illumination, both light paths are used.

Much effort has been made to improve the accuracy of the setup. A class-A spectrum of the front and rear illumination was ensured by adapting the spectral filters in front of the flash lamp. The uniformity of the front and rear irradiance in the solar cell plane was measured to be better than classification A. To furthermore prevent light

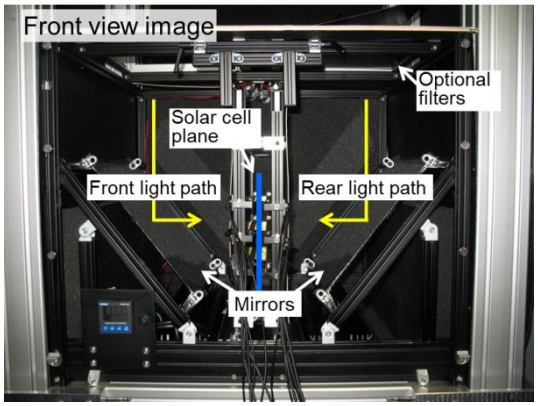

Figure 5: Front view image of the two-mirror setup used in this study for measuring the *IU* characteristics of bifacial solar cells with single- and both-sided illumination (front lid opened).

from passing from one side to the other side of the solar cell, non-reflective, moveable apertures were installed, which can be moved very close to the edges of the solar cell from all sides. Seven mesh filters with transmittances in the range of 10 to 40 % are available to reduce the irradiance onto the rear side of the solar cell in a spectrally neutral way [23]. For this purpose, the filters are placed into the rear light path.

A temperature regulation unit and an isolating enclosure are used to stabilize the temperature of the bifacial solar cell to 25.0 ± 0.3°C. Calibrated tactile Pt100 sensors have been installed on a central busbar in a non-destructive way [24] to track the solar cell temperature during measurements.

To mitigate hysteresis effects, the voltage sweep is separated into multiple segments by applying multiple flashes. Forward and backward sweeps were performed and the average is determined.

Finally, the spectral mismatch between monitor solar cell and front side of the bifacial solar cell is evaluated for each cell to avoid mismatch errors during equivalent irradiance measurements. Because of the application of a spectrally matched monitor cell, the spectral mismatch changes by less than 0.02%$_{rel}$ for the bifacial PERC cells of this study.

3.4 Calibration of Front and Rear Irradiances

In addition to the constructional optimization of the setup, the measurement procedure and the calibration of the two-mirror setup have been evaluated thoroughly to further improve accuracy.

Prior to the measurements at the two-mirror setup, the spectral responsivity and the *IU* characteristics of front and rear side of the bifacial solar cells are measured at conventional, well-established setups at CalLab PV Cells [17,25] on non-reflective chucks.

Calibration of front irradiance:

$I_{sc,front,STC}$ measured at the conventional sun simulator has been used to calibrate the front irradiance of the two-mirror setup to standard testing conditions. By using a blocking lid for the rear light path, the intensity of the flash light source of the two-mirror setup is adjusted until the measured front side short-circuit current matches $I_{sc,front,STC}$.

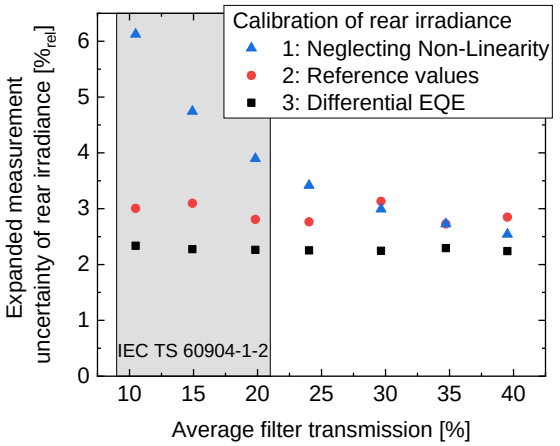

Figure 6: Expanded measurement uncertainty of rear irradiance (coverage factor of 2) as a function of filter transmission for the three different calibration procedures. The mesh filters covered by the IEC technical specification 60904-1-2 are marked by the grey-shaded area.

Calibration of rear irradiance:

Three different approaches for the calibration of rear irradiance have been evaluated.

(1) *Neglecting nonlinearity:* After calibration of the front irradiance, the front light path is blocked and a mesh filter with transmittance in the range of 10 to 40 % is installed in the rear light path. The rear short-circuit current $I_{sc,rear}$ is measured with these illumination conditions. E_{rear} is determined from the equation $E_{rear} = I_{sc,rear}/I_{sc,rear,STC} \cdot 1000\ W/m^2$, which assumes linearity.

(2) *Using reference data:* After calibration of the front irradiance, the rear irradiance is determined by calculation using reference values for the average filter transmission and the spectral mismatch between front and rear side of the bifacial cell.

(3) *Using differential EQE calibration:* After calibration of the front irradiance, the rear current is measured with the front light path blocked and a mesh filter installed. The exact relation between rear short-circuit current $I_{sc,rear}$ and rear irradiance E_{rear} determined by differential EQE measurements is used (*c.f.* Figure 2)..

The expanded measurement uncertainty of the rear irradiance has been evaluated for the three calibration approaches, see Figure 6.

Neglecting nonlinearity leads to rather high measurement uncertainties due to the high impact of nonlinearity at low irradiance levels (*c.f.* Figure 2). For higher filter transmission, the uncertainty of $I_{sc,rear,STC}$ measured at the conventional setup is the main contribution.

Using reference data for the calibration of E_{rear} yields medium measurement uncertainties, with the uncertainty of $I_{sc,front,STC}$, the uncertainty of difference in shading by front and rear contact bars and the uncertainty of the average filter transmission being the main contributions.

For the approach using differential EQE calibration, the main contribution to the E_{rear} uncertainty comes from the uncertainty of the differential EQE measurements. As the approach directly accounts for linearity of the bifacial solar cells, it yields the lowest uncertainty of all

calibration approaches and therefore has been applied for the measurement of bifacial cells with both-sided illumination.

3.5 Measurement Accuracy of the Two-Mirror Setup

To assess the measurement accuracy of the two-mirror setup, Monte Carlo simulations [26] of the measurement uncertainties of front, rear and equivalent irradiance as well as the corresponding *IU* characteristics have been carried out. Correlations between different uncertainty contributions have been taken into account.

Figure 7 shows the expanded measurement uncertainties for short-circuit current u_{Isc} and maximum power u_{Pmpp} for the different mesh filters. The most significant contribution to u_{Isc} and u_{Pmpp} comes from the measurement uncertainty of $I_{sc,front,STC}$ determined at the conventional sun simulator. As this uncertainty contributes to all filters alike, u_{Isc} and u_{Pmpp} only depend slightly on the filter transmission.

By adapting the contact bars to reduce voltage distribution over the busbars [27], the measurement uncertainties for P_{mpp} will be reduced to 1.5 % in the near future.

For comparing bifacial and G_E methods, the difference in *IU* parameters between the two methods is calculated. As both methods are applied at the same setup with the same calibration procedure, the most significant contributions to the measurement uncertainty –*e.g.* the measurement uncertainty of $I_{sc,front,STC}$– are correlated and cancel out. The differences in the *IU* parameters between the methods can thus be measured with much higher accuracy than the respective *IU* parameters themselves. Monte Carlo simulations of the expanded measurement uncertainty of the difference have been carried out, see Figure 7. The measurement uncertainties for the differences in I_{sc} and P_{mpp} are only one-third of u_{Isc} and u_{Pmpp}. This way, the difference in I_{sc} and P_{mpp} can be measured with expanded uncertainties in the range of 0.24 to 0.36 % and 0.53 to 0.59 %, respectively, for the filter configurations specified by IEC TS 60904-1-2.

4 COMPARISON OF *IU* MEASUREMENTS WITH SINGLE- AND BOTH-SIDED ILLUMINATION

4.1 Comparison at Front Irradiance of 1000 W/m^2

The *IU* characteristics of a nonlinear bifacial PERC solar cell have been measured using both bifacial and G_E methods. Thereby, mesh filters have been used to reduce the irradiance onto the rear side for the bifacial method. The measured I_{sc} and P_{mpp} values and the difference between bifacial and G_E methods including the corresponding expanded uncertainties are shown in Figure 8. *IU* measurements of other bifacial PERC cells yield similar differences.

It can be seen that I_{sc} and P_{mpp} increase with increasing rear irradiance and equivalent irradiance, respectively. The differences between both methods are below 0.05 %$_{rel}$ for I_{sc} and 0.1 %$_{rel}$ for P_{mpp}, which is clearly within the corresponding measurement uncertainties. This leads to the conclusion that the two methods presented in the IEC technical specification 60904-1-2 are indeed consistent for bifacial solar cells with respect to nonlinearity.

The authors like to point out that there are additional effects on the module level which may lead to a higher

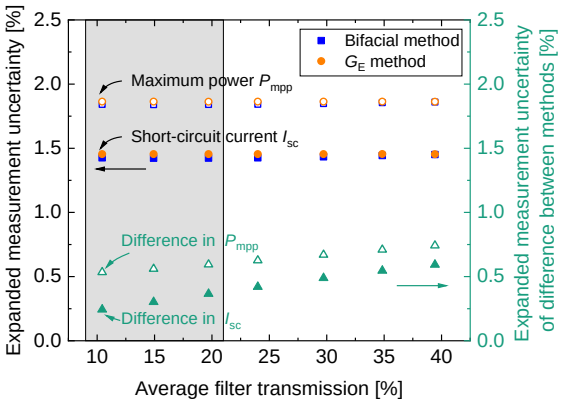

Figure 7: Expanded measurement uncertainty of short-circuit current u_{Isc} (closed symbols) and maximum power u_{Pmpp} (open symbols) for bifacial and G_E methods (coverage factor of 2). The uncertainties have been determined by Monte Carlo simulations. The uncertainties for the differences between the two methods have also been determined under consideration of correlations and are shown as green triangles. The mesh filters covered by the IEC technical specification 60904-1-2 are marked by the grey-shaded area.

difference between bifacial and G_E methods for bifacial modules. Current mismatch between different cells under rear illumination or partial shading of the rear by the junction box, cables or module frames can lead to significant differences between the two methods. For assessing bifacial solar cells, these effects are not relevant though.

4.2 Comparison at Lower Front Irradiances

In field operation, irradiances onto bifacial devices can be significantly smaller than 1000 W/m^2 [28]. For lower total irradiances, the influence of nonlinear recombination characteristics or inversion layer shunting becomes stronger. In this study, bifacial and G_E methods have therefore also been compared for reduced E_{front} using generalized measurement methods.

Generalized bifacial method: The bifacial solar cells have been illuminated with front irradiance E_{front} and simultaneous rear irradiance of $f_{rear} \cdot E_{front}$ with f_{rear} = 0.1 and 0.2, respectively, standing for the rear irradiance ratio.

Generalized equivalent irradiance method: Front illumination only with equivalent irradiance

$$E_E = E_{front} \cdot \left(1 + \frac{I_{sc,rear,Efront}}{I_{sc,front,Efront}} \cdot f_{rear}\right), \quad f_{rear} = 0.1 \text{ and } 0.2$$

has been used. Thereby, $I_{sc,rear,Efront}$ and $I_{sc,front,Efront}$ denote the rear and front short-circuit current measured at rear and front side irradiance E_{front}, respectively. This generalized formula implies that the share of rear to front irradiance is constant and the rear irradiance directly scales with front irradiance.

For the calculation of the generalized equivalent irradiance, it is important to evaluate the I_{sc} ratio at E_{front}. Evaluating the ratio at another irradiance level, *e.g.* at the "standard" irradiance of 1000 W/m^2, can lead to significant overestimation of E_E, as the I_{sc} ratio strongly depends on irradiance for nonlinear bifacial solar cells (*c.f.* Figure 3).

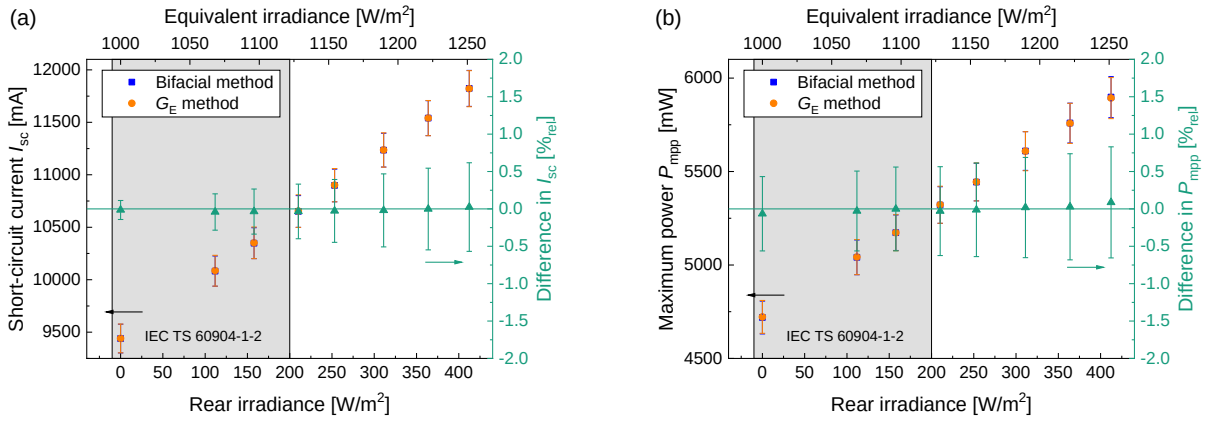

Figure 8: Measured (a) short-circuit current I_{sc} and (b) maximum power P_{mpp} for different rear irradiances with the bifacial method using both-sided illumination (blue squares) or different equivalent irradiance levels with the G_E method using front side illumination only (orange circles). The difference between bifacial and G_E methods is shown as green triangles on the right axes. The measurements have been performed with randomized variation of irradiance levels. Error bars show the expanded measurement uncertainties with coverage factor of 2. Illumination conditions covered by the IEC technical specification 60904-1-2 are marked by grey-shaded areas.

In this study, nonlinear bifacial PERC solar cells have been measured with generalized bifacial and G_E methods applying front irradiance levels of 200 and 500 W/m^2 in addition to the standard irradiance of 1000 W/m^2.

The measured differences in short-circuit current I_{sc} between the bifacial and G_E methods are shown in Figure 9. It can be seen that the difference is slightly higher for the lower front irradiance, but still within the uncertainty of the standard measurement. As the measurement uncertainties for lower irradiance have not yet been derived, the consistency of the bifacial and G_E methods could not be finally proven though. Nevertheless, it is expected that the relative measurement uncertainties for lower irradiance levels will be comparable or higher than for the standard irradiance. Additionally, there are further strong indications for consistency: PC1D simulations yield comparable –and insignificant– I_{sc} differences for all irradiance levels.

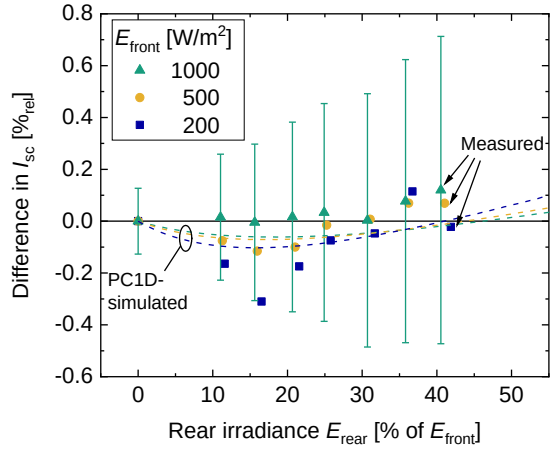

Figure 9: Measured (symbols) and PC1D-simulated (dashed lines) difference in short-circuit current I_{sc} between bifacial and G_E methods for different front irradiances. For reasons of clarity, the rear irradiance is given in terms of E_{front}.

This study therefore suggests that the bifacial and G_E methods are consistent for various irradiance levels, also for nonlinear bifacial cells.

5 SUMMARY

In this study, the consistency of the bifacial method and the equivalent (G_E) irradiance method, which have been proposed in the IEC technical specification (TS) 60904-1-2 for characterisation of bifacial solar devices, is evaluated for bifacial solar cells in detail. Differences in the current-voltage (*IU*) characteristics between both methods are investigated by simulations and measurements for bifacial solar cells with nonlinear relation of short-circuit current and irradiance.

To be able to detect differences between the methods with highest accuracy, the setup for the *IU* measurements of bifacial solar cells has been comprehensively overhauled. The homogeneity and spectral distribution of front and rear irradiance has been improved to surpass classification A. A temperature regulation unit has been implemented to precisely control the cell temperature. Additionally, a monitor solar cell that spectrally matches the front of the bifacial solar cell has been applied. Finally, different approaches for the calibration of rear irradiance have been evaluated and the procedure with lowest measurement uncertainty identified and established.

The measurement uncertainties for the *IU* parameters of both bifacial and G_E methods have been determined by means of Monte Carlo simulations taking into account correlations between the different contributions. As both measurements are applied at the same setup, the difference between the two methods can be measured with high precision because significant contributions to the measurement uncertainty cancel out. The difference in I_{sc} and P_{mpp} can be measured with expanded uncertainties in the range of 0.24 to 0.36 % and 0.53 to 0.59 %, respectively, for the configurations specified by IEC TS 60904-1-2.

The *IU* characteristics of bifacial passivated emitter and rear (PERC) solar cells with silicon oxynitride/silicon

nitride (SiO_xN_y/SiN_z) rear surface passivation have been measured with this setup. To the authors' knowledge, no bifacial solar cells with stronger nonlinearity are currently available, so that this study represents a worst-case investigation.

At 1000 W/m^2 front irradiance, differences in *IU* parameters between the two methods were measured to be below 0.1 %$_{rel}$, which is clearly within the corresponding measurement uncertainties. The two methods presented in the IEC technical specification 60904-1-2 can therefore indeed be considered as consistent on solar cell level, also for bifacial solar cells with strong nonlinearity. In field operation, front irradiance is generally lower than 1000 W/m^2 as proposed by the IEC TS. Both measurements and PC1D simulations suggest that bifacial and G_E methods are consistent for these illumination conditions as well. For bifacial solar modules, additional module-specific contributions may lead to higher differences.

Although nonlinearity can be excluded as source of difference between bifacial and G_E methods for present bifacial solar cell types, further peculiarities may lead to differences for upcoming types. It is thus advisable to test bifacial solar cells for consistency of the two methods. CalLab PV Cells offers these tests as service measurements with high accuracy.

6 ACKNOWLEDGEMENTS

This project has received funding from the EMPIR programme co-financed by the Participating States and from the European Union's Horizon 2020 research and innovation programme within the project "PV-Enerate" (number 16ENG02).

This work has been partly supported by the German Federal Ministry for Economic Affairs and Energy within the project "BiZePS" (contract number 0325909).

7 REFERENCES

[1] International Technology Roadmap for Photovoltaic (ITRPV), Results 2018, 10th Edition (2019).

[2] International Electrochemical Commission, *IEC 60904: Photovoltaic devices – Part 1-2: Measurement of current-voltage characteristics of bifacial photovoltaic (PV) devices*, Technical Specification, 2019.

[3] A. Schmid, G. Dülger, G. Baraah, *et al.*, *IV Measurement of Bifacial Modules: Bifacial vs. Monofacial Illumination*, Proc. 33rd EUPVSEC, Amsterdam, The Netherlands, (2017), 1624.

[4] G. Arnoux, N. Bassi, V. Fakhfouri, *et al.*, *Toward the standardisation of the power rating of bifacial solar cells*, presented at 13th SNEC conference, Shanghai, China, 2018.

[5] C. Deline, S. MacAlpine, B. Marion, *et al.*, *Assessment of Bifacial Photovoltaic Module Power Rating Methodologies—Inside and Out*, IEEE Journal of Photovoltaics Vol. 7, No. 2 (2017): 575-580.

[6] L. Peyrot, G. Razongles, L. Sicot, *et al.*, *Bifacial Module Measurements with G_E Method*, presented at 4th bifiPV workshop, Constance, Germany, 2017.

[7] J. P. Singh, T. M. Walsh, A. G. Aberle, *A new method to characterize bifacial solar cells*, Prog. Photovolt: Res. Appl. 2012; 22: 903-909.

[8] A. G. Aberle, S. Glunz, W. Warta, *Impact of illumination level and oxide parameters on Shockley–Read–Hall recombination at the Si-SiO_2 interface*, J. Appl. Phys. 71 (91), 1992; 4422.

[9] S. Dauwe, L. Mittelstädt, A. Metz, *et al.*, *Experimental Evidence of Parasitic Shunting in Silicon Nitride Rear Surface Passivated Solar Cells*, Prog. Photovolt: Res. Appl. 2002; 10:271–278.

[10] Y. Hishikawa, H. Shimura, Y. Ishii, *et al.*, *Measurement procedure for bifacial PV devices*, presented at 3rd bifiPV workshop, Miyazaki, Japan, 2016.

[11] P. Palinginis, C. Kusterer, S. Steckemeth, *et al.*, *Pioneering the industrialization of PERC technology: A review of the development of mono- and bifacial PERC solar cells at SolarWorld*, Photovoltaics International, Edition 42, 2019: 51-72.

[12] J. Seiffe, L. Gautero, M. Hofmann, *et al.*, *Surface passivation of crystalline silicon by plasma-enhanced chemical vapor deposition double layers of silicon-rich silicon oxynitride and silicon nitride*, J. Appl. Phys. **109**, 034105 (2011).

[13] M. Müller, G. Fischer, B. Bitnar, *et al.*, *Loss analysis of 22% efficient industrial PERC solar cells*, Energy Procedia 124 (2017) 131–137.

[14] J. Metzdorf, S. Winter, T. Wittchen. *Radiometry in photovoltaics: calibration of reference solar cells and evaluation of reference values*, Metrologia 37.5 (2000): 573.

[15] J. Hohl-Ebinger, G. Siefer, W. Warta, *Non-linearity of Solar Cells in Spectral Response Measurements*, Proc. 22nd EUPVSEC, Milan, Italy, (2007), 422.

[16] K. Bothe, D. Hinken, B. Min, et al., *Accuracy of Simplifications for Spectral Responsivity Measurements of Solar Cells*, IEEE Journal of Photovoltaics Vol. 8, No. 2 (2018): 611-620.

[17] J. Hohl-Ebinger, W. Warta, *Bifacial solar cells in STC measurement*, Proc. 25th EUPVSEC, Valencia, Spain, (2010), 1358.

[18] M. Rauer, K. Bothe, C. Comparotto, *et al.*, *Monofacial IV Measurements of Bifacial Silicon Solar Cells in an Inter-Laboratory Comparison*, Proc. 32nd EUPVSEC, Munich, Germany, (2016), 915.

[19] J. Metzdorf, *Calibration of solar cells. 1: The differential spectral responsivity method*, Applied Optics 26.9 (1987): 1701-1708.

[20] M. Rauer, J. Greulich, N. Wöhrle, *et al.*, *Bifacial Solar Cells under Single- and Double-Sided Illumination: Effect of Non-Linearity in Short-Circuit Current*, presented at 4th bifiPV workshop, Constance, Germany, 2017.

[21] H. Ohtsuka, M. Sakamoto, M. Koyama, et al., *Characteristics of Bifacial Solar Cells Under Bifacial Illumination with Various Intensity Levels*, Prog. Photovolt: Res. Appl. 2001; 9:1-13.

[22] M. Ezquer, I. Petrina, J. M. Cuadra, et al., *Design of a Special Set-up for the I-V Characterization of Bifacial Photovoltaic Solar Cells*, Proc. 23rd EUPVSEC, Valencia, Spain, (2008), 1553.

[23] A. A. Santamaría, G. Bardizza, H. Müllejans, *Assessment of uncalibrated light attenuation filters constructed from industrial woven wire meshes for*

use in photovoltaic research, Proc. 29th EUPVSEC, Amsterdam, The Netherlands, (2014), 3214.

[24] A. Edler, M. Schlemmer, J. Ranzmeyer, et al., *Flasher setup for bifacial measurements*, presented at 1st bifiPV workshop, Constance, Germany, 2012.

[25] J. Hohl-Ebinger, *Untersuchungen zur hochpräzisen Vermessung der elektrischen Parameter von Solarzellen*, Dissertation, University of Constance, 2011.

[26] Joint Committee for Guides in Metrology (JCGM), *Evaluation of measurement data – Supplement 1 to the "Guide to the expression of uncertainty in measurement" – Propagation of distributions using a Monte Carlo method*, JCGM 101:2008.

[27] S. K. Reichmuth, M. Rauer, J. Hohl-Ebinger, *Progress in Contacting Silicon Solar Cells with Complex Metallization Layout for I-V Measurements*, presented at 46th IEEE PVSC, Chicago, USA, 2019.

[28] U. A. Yusuglofu, T. M. Pletzer, L. J. Koduvelikulathu, et al., *Analysis of the Annual Performance of Bifacial Modules and Optimization Methods*, IEEE Journal of Photovoltaics Vol. 5, No. 1 (2015): 320-328.